Journal of the Korean Physical Society, Vol. 53, No. 2, August 2008, pp. 851∼862

Stochastic Modeling of External Electric Field Effect on *Escherichia Coli* Min Protein Dynamics

Charin Modchang, Wannapong Triampo,* Paisan Kanthang,
Udorn Junthorn, Somrit Unai, Waipot Ngamsaad and Narin Nuttavut
R&D Group of Biological and Environmental Physics (Biophysics), Department of Physics, Faculty of Science, Mahidol University, Bangkok, Thailand
Center of Excellence for Vector and Vector-Borne Diseases, Mahidol University, Bangkok, Thailand and Institute for Innovation and Development of Learning Process, Mahidol University, Bangkok, Thailand

Darapond Triampo
Department of Chemistry, Faculty of Science, Mahidol University, Bangkok, Thailand

Yongwimon Lenbury
Department of Mathematics, Faculty of Science, Mahidol University, Bangkok, Thailand

(Received 28 November 2007, in final form 16 April 2008)

Cell division in *Escherichia coli* and other rod-shaped bacteria depends on the precise placement of a division septum at the cell center. The MinCDE system consisting of three proteins, MinC, MinD, and MinE, controls accurate cell division at the center of the cell through pole-to-pole oscillation. With simplifying assumptions and relying on a deterministic model, we present a one-dimensional stochastic model that describes the effects of an external electric field on the MinCDE system. Computer simulations were performed to investigate the response of the oscillatory dynamics to various strengths of the electric field and to the total number of Min proteins. A sufficient electric field strength was capable of interfering with MinCDE dynamics with possible changes to the cell division process. Interestingly, effects of an electric field were found not to depend on the total number of Min proteins. The noise involved shifted the correct trend of Min proteins behavior. However, as a consequence of the robustness of the dynamics, the oscillatory pattern of the proteins still existed even though the number of Min proteins was relatively low. When considering the correlations between the local and the global minimum (maximum) of MinD (MinE), the results suggest that using a high enough Min protein concentration will reduce the local minimum (maximum) effect, which is related to the probability of polar division in each single oscillator cycle. Although this model is simple and neglects some complex mechanisms concerning protein oscillation in correlation with cell division, it has been demonstrated to be good enough for positioning of the dividing site. Nevertheless, more experimental and theoretical studies are needed to provide a more realistic (but of course more complicated) model of bacterial cell division.

PACS numbers: 87.15.Aa
Keywords: Electric fields, *E. coli*, Cell division, Min proteins, MinCDE oscillation, Stochastic process

I. INTRODUCTION

The dynamics of Min proteins, MinCDE, consisting of three proteins, namely, MinC, MinD, and MinE, plays a key role in determining the site of septal placement in *Escherichia coli* [1]. MinC and MinD act in concert to form a nonspecific inhibitor of septation, and MinC also interacts with the division protein FtsZ to prevent formation of a stable FtsZ ring marking the dividing site [2]. In other words, MinC is an antagonist of FtsZ polymerization and a specific inhibitor of Z-ring formation [2, 3], while MinD makes MinC-mediated inhibition of cell division sensitive to suppression by MinE [4]. The division inhibitor MinCD lacks site specificity, as evidenced by the observation that expression of MinC and MinD in the absence of MinE leads to a block in septation at all potential division sites, leading to formation of long nonseptate filaments. Filament formation is suppressed by MinE, which acts as a topological specificity factor

*E-mail: scwtr@mahidol.ac.th; wtriampo@gmail.com;
Tel: +662-441-9816(ext.1131); Fax: +662-441-9322;
R&D Group of Biological and Environmental Physics, Department of Physics, Faculty of Science, Mahidol University, Rama 6 Rd., Ratchatewee, Bangkok, 10400 Thailand

to prevent MinCD from acting at the midcell site while permitting it to block septation at polar division sites. MinD localizes to the cell pole in a MinE-dependent fashion and undergoes a rapid oscillation from pole to pole [5].

The necessity for quantitative modeling and simulation is especially compelling when the process of interest displays a spatiotemporal pattern formation, such as the oscillations of Min proteins. Several studies have been made employing different reaction-diffusion models to explain these oscillations [6–10]. Incorporating stochastic features into Min modeling is, nevertheless, likely to be important for systems of this type [9,11–14]. Ngammsaad *et al.* [15] mesoscopically applied lattice a Boltzmann technique, and more recently Modchang *et al.* [16] deterministically investigated these MinCDE dynamics under an external electric field.

Given the significance of protein oscillation in regulating cell division, it is of interest to understand how abnormal or unsuccessful cell division is affected by abnormal protein oscillation. More specifically, under an external perturbation, pH, heat, electric field, or magnetic field, of such stress, how does each perturbation or combined perturbation affect protein oscillation and cell division? In this study we have focused on the effect of the electric field because proteins are charged and, thus, should interact with the electric field [17].

MinCDE are membrane-bound proteins and can diffuse in the cytoplasm as well as within the plane of membrane. Given a high enough electric field, the movements of these proteins should be perturbed. Here, we have tested the hypothesis that a small direct current (dc) induced physiological electric field can perturb *E. coli* cell division via changes in the protein is dynamic oscillation. The relative concentrations of MinD and MinE were reported as functions of space and time, and for each Min protein species considered, the characteristic model parameters, field strength J and number of Min proteins, were varied and comparatively interpreted. We also present a simple one-dimensional stochastic model that predicts the experimental observations of Min protein oscillations. The stochastic modeling approach is used in order to take into account fluctuations or noises.

II. RATIONALE MODEL OF PROTEIN OSCILLATORY PERTURBATION UNDER AN EXTERNAL ELECTRIC FIELD

Studies of the response of living systems to uniform physical fields (electric, gravitational, and magnetic) are capable of yielding novel insights into a variety of biological processes [18–22]. In particular, direct current electric fields are able to induce directional responses, such as cell division of many cell types [22–24]. For example, Zhao *et al.* [22] showed that application of static electric fields to dividing human corneal epithelial cells causes division planes to orient [25].

Electrical phenomena govern many biological processes from molecular binding interactions to intercellular communication. Endogenous or exogenous perturbations of small extracellular electric fields have been observed to affect cellular processes, and several different mechanisms for these effects have been proposed [26]. Diverse biological responses to electric fields continue to motivate experimental searches for mechanisms of electromagnetic interactions with cells. Cell development [27], regeneration [28–30], and repair [31] are all effected by electric fields, and many other basic cellular functions, including motility [32–34] and receptor regulation [35], are modulated by applied external electric fields. In addition, cell membrane permeabilization and fusion are affected by applied fields [36–38]. Local perturbation of plasma membrane potentials provides a hypothetical mechanism of interaction of applied electric fields with cells. Electric fields of high strength applied as short time pulses (microsecond) to aqueous suspensions of living cells have remarkable effects on the cell membranes and can even kill the organisms. Electric fields can be applied to cell suspensions by the use of capacitor discharges as a part of a high voltage circuit [39,40]. Sinusoidal electric fields can alter fundamental cellular functions [41], and this has led to concerns of the potential biological hazards resulting from exposure to environmental sinusoidal fields. Most of the proposed coupling mechanisms are the subject of substantial debate.

The possibility of applying low-intensity electricity has been studied because of its effects on viable microbial interactions [42,43]. Studies of the effects of application of a high-voltage electric current (intensity > 25 kW cm^{-1}) on microorganisms have been carried out on different yeast and bacterial species [44]. There was a notable reduction in the viability of bacterial cultures, indicating that this is due to chemical reactions induced by the electric treatment [45]. However, the behavior of a single cell or cell clusters in an external electric field has not been thoroughly investigated. Moreover, no study has been performed to assess the effects of an electric field on the oscillatory dynamics of protein within a cell, either theoretically or experimentally.

We hypothesize that a bacterium (*E. coli*) cell membrane may act as a "shield" or "absorber" to the cytoplasmic organelles, including cytoplasmic and membrane-bound Min proteins. It is possible that an applied electric field will eventually penetrate the membrane and interact with these interior components of the cell and, consequently, generate an electric force on charged objects (viz. Min proteins). It is important to note that, if the field is too strong, the cell membrane may be damaged, possibly resulting in cell death or abnormality [37, 42, 45, 46]. Another possible factor is the generation of an induced secondary field. A high enough field strength could polarize or redistribute the somewhat mobile charges. With this induced polarization, it is possible to generate a secondary field inside *E. coli*

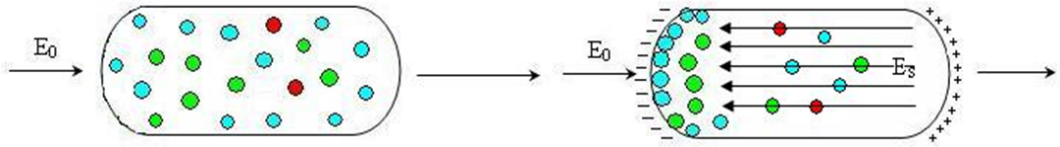

Fig. 1. Dielectric-like *E. coli* cell in a uniform field E_0, showing the polarization on the left and the polarization charge with its associated, opposing electric field on the right.

in a direction parallel, but opposite, to the direction of the primary applied field. This is based on the assumption that the cell membrane is a dielectric material as shown in Figure 1. It has been shown previously that the dielectric properties of these membranes are highly characteristic of, and rapidly affected by, alterations in physiological activities and induction of pathologic states in cells [47–53]. Such differences can be used not only for cell characterization but also for exploitation to selectively manipulate, separate, and sort cells [53–56]. This situation is, in fact, very complicated and highly dependent on the electrolytic conditions. Even in the absence of an external electric field, particles exposed to an ion cloud become charged. Ions will collide with a particle due to their thermal motions. As the particle becomes charged, it will repel ions of the same charge, leading to a nonhomogenous distribution of ions in its neighborhood. These phenomena can be viewed as a nonlinear feedback. However, in our model, we will assume that this effect is negligible as far as the protein oscillatory behavior is concerned.

With the rapid development of dielectric spectroscopy and AC electrokinetic methods, various supramolecules and biological cells have been studied [57–59]. To analyze the dielectric behavior of *E. coli* cells in suspension, Asami *et al.* [60] developed a theory based on a two-shell spheroidal model. The cell model assumed the *E. coli* cell to be an ellipsoid covered with two confocal shells corresponding to the plasma membrane and the cell wall. More recently, Hölz [61] in studying the dielectric properties of *E. coli* cells by means of electrorotation estimated the electrical parameters of the cellular components using a three-shell spherical model that included the periplasmic space between the outer and the inner membranes.

III. STOCHASTIC MODEL

Here, we present a simple one-dimensional stochastic model that predicts Min-protein oscillations in *E. coli*. Based on our deterministic model at the mean-field level [16], the dynamics of these Min proteins in the presence of an external field are described by

$$\frac{\partial \rho_D}{\partial t} = D_D \frac{\partial^2 \rho_D}{\partial x^2} + J_D \frac{\partial \rho_D}{\partial x} - \frac{\sigma_1 \rho_D}{1+\sigma_1' \rho_e} + \sigma_2 \rho_e \rho_d \ , \quad (1)$$

$$\frac{\partial \rho_d}{\partial t} = D_d \frac{\partial^2 \rho_d}{\partial x^2} + J_d \frac{\partial \rho_d}{\partial x} + \frac{\sigma_1 \rho_D}{1+\sigma_1' \rho_e} - \sigma_2 \rho_e \rho_d \ , \quad (2)$$

$$\frac{\partial \rho_E}{\partial t} = D_E \frac{\partial^2 \rho_E}{\partial x^2} + J_E \frac{\partial \rho_E}{\partial x} - \sigma_3 \rho_D \rho_E + \frac{\sigma_4 \rho_e}{1+\sigma_4' \rho_E} \ , \quad (3)$$

and

$$\frac{\partial \rho_e}{\partial t} = D_e \frac{\partial^2 \rho_e}{\partial x^2} + J_e \frac{\partial \rho_e}{\partial x} - \sigma_3 \rho_D \rho_E - \frac{\sigma_4 \rho_e}{1+\sigma_4' \rho_D} \quad (4)$$

where ρ_D and ρ_E are the concentrations of the MinD and the MinE proteins in the cytoplasm respectively, and ρ_d and ρ_e are the concentrations of the MinD and the MinE roteins on the cytoplasmic membrane. The first equation describes the rate of change with time of the concentration of MinD (ρ_D) in cytoplasm. The second equation describes the time rate of change of the MinD concentration (ρ_d) on cytoplasmic membrane. The third equation and the fourth equation describe the corresponding rate of change for MinE (ρ_E) in the cytoplasm and on the cytoplasmic membrane, respectively. The external field parameter J_i describes the strength of an applied electric field. The constant σ_1 represents the spontaneous association of MinD to the membrane wall [62] whereas the constant σ_2 describes the release of MinD from the cell membrane by membrane-bound MinE. Similarly, the constant σ_3 describes the recruitment of cytoplasmic MinE to the membrane by cytoplasmic MinD, and the constant σ_4 represents the spontaneous membrane dissociation of MinE [63]. The constant σ_1' corresponds to membrane-bound MinE suppression of the binding of MinD to the membrane, and σ_4' corresponds to that of cytoplasmic MinD suppression of the release of the membrane-bound MinE. As previous experimental results showed that MinC dynamics followed that of the MinD protein [64], for the sake of simplicity, consideration of MinC dynamics is, therefore, omitted. In this model, we adopt a dynamic model of compartmentalization in the bacterial cell division process [6,9] (schematically represented in Figure 2) by adding an extra term, $J_i\ (\partial \rho_i / \partial x)$, that depends on the external electric field.

To investigate how the intrinsic chemical fluctuations in spatially extended systems can give rise to properties radically different from what would be described by a mean-field model in the Min protein systems, we modified our deterministic model [16] to a discrete particle model, where the Min protein molecule is represented as a particle that may hop between lattices. The number of protein molecules at site k is n_i^k, with $i =$

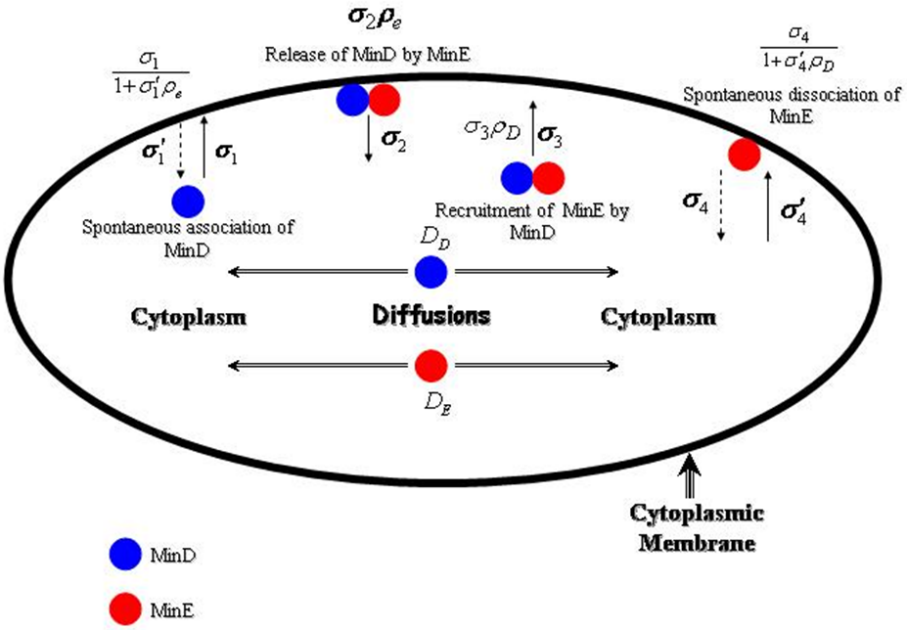

Fig. 2. Schematic diagram of MinCDE dynamics.

$\{D, d, E, e\}$ representing cytoplasmic MinD, membrane-bound MinD, cytoplasmic MinE, and membrane-bound MinE, respectively. Here, the dynamics of Min protein system is a reaction-diffusion system consisting of two processes: The first is a diffusion process that describes diffusion of the Min proteins, which results in a net flow of chemical species from regions of higher concentration to regions of lower concentration and the second one is a reaction process that describes self-organization of biological systems.

With regards to the diffusion process, in the absence of an external electric field, at each time period Δt, these particles have an equal probability $D_i\Delta t/(\Delta x)^2$ to hop to one of their neighboring sites with lattice space Δx and time step Δt. When the external electric field is present, the probability for a particle to hop to the left or to the right neighboring site is no longer equal, but, in this case, it becomes

$$\begin{aligned} P_L &= \frac{D_i\Delta t}{(\Delta x)^2}\left(0.5+\frac{J_i\Delta t}{2\Delta x}\right); \\ P_R &= \frac{D_i\Delta t}{(\Delta x)^2}\left(0.5-\frac{J_i\Delta t}{2\Delta x}\right) , \end{aligned} \tag{5}$$

where P_L, and P_R are the probabilities for a particle to hop to the left and to the right neighboring site, respectively, and J_i is an external field parameter. We assume that a chemical substance moving in the region of an external field will experience a force that is proportional to the external field parameter J_i. In general, $J_i = \mu_i E$, $i = \{D, d, E, e\}$, where E is the strength of the field in the cytoplasm and μ is the ionic mobility of the chemical substance, which is proportional to the diffusion coefficient and depends on the total amount of charge on that substance.

With regards to the reaction process, at site k, the following reactions may occur:

	Probability:
$n_D^k \to n_D^k - 1, n_d^k \to n_d^k + 1$	$P_{D\to d} = \sigma_1\Delta t/(1+\sigma_1' n_e^k)$,
$n_D^k \to n_D^k + 1, n_d^k \to n_d^k - 1$	$P_{d\to D} = \sigma_2\Delta t n_e^k$,
$n_E^k \to n_E^k - 1, n_e^k \to n_e^k + 1$	$P_{E\to e} = \sigma_3\Delta t n_D^k$,
$n_E^k \to n_E^k + 1, n_e^k \to n_e^k - 1$	$P_{e\to E} = \sigma_4\Delta t/(1+\sigma_4' n_D^k)$.

The first (third) reaction indicates that each MinD (MinE) molecule at site k in the cytoplasm may bind to the cell membrane with equal probability $P_{D\to d}(P_{E\to e})$, and the second (fourth) reaction indicates that each membrane-bound MinD (MinE) molecule at site k may be released to the cytoplasm with equal probability $P_{d\to D}(P_{e\to E})$. These reactions are stochastic analogs of the reaction processes in our deterministic model [16]. Since protein synthesis can be blocked without affecting protein oscillation [65], we do not include protein synthesis or degradation in our model. We also assume that the total amounts of MinD and MinE are unchanged.

IV. SIMULATIONS, CONDITIONS, AND PARAMETERS

In our simulation, we use lattice space $\Delta x = 0.02$ μm and time step $\Delta t = 2 \times 10^{-4}$ s. The length of *E. coli* is taken to be 2 μm, and there are 100 lattice sites within the bacterium. The numerical values of our parameters have not been experimentally determined for the Min proteins. We chose a cytoplasmic diffusion constant of

Table 1. Scaled parameters used in the simulations.

N	σ_1'	$\sigma_2(s^{-1})$	$\sigma_3(s^{-1})$	σ_4'
200	25.0	0.27	30.0	20.0
400	2.0	0.135	15.0	10.0
800	0.6	0.0675	7.5	5.0
1500	0.25	0.036	4.0	2.7

slightly less than the value 2.5 μm^{2}s^{-1} determined for a maltose binding protein in *E. coli* cytoplasm [65]. The other reaction rate parameters are chosen to fit the results of the model with the experimental results for no external field, particularly for the oscillation period and oscillation pattern. However, we emphasize that our results for the oscillatory behavior observed below are typical for large regions of the parameter space, with or without the external field effect. We have used $D_D = 0.28$ μm^{2}s^{-1}, $D_d = 0.003$ μm^{2}s^{-1}, $D_E = 0.6$ μm^{2}s^{-1}, $D_e = 0.006$ μm^{2}s^{-1}, $\sigma_1 = 20$ s^{-1} and $\sigma_4 = 0.8$ s^{-1} [6, 9]. To determine the effect of an external electric field on the oscillatory behaviors with changes in the number of Min proteins, we used four representative parameter sets (shown in Table 1), where N is the total number of MinD, which is equal to the total number of MinE. We used equal numbers of Min proteins because "wild-type" oscillations are observed when both plasmid-encoded proteins are equally expressed [66]. To preserve the strength of the interaction between Min proteins when the total number of Min proteins is changed, we scaled the four parameters σ_1', σ_2, σ_3 and σ_4' (Table 1) [9].

In general, the ionic mobility (or electrophoretic mobility) of the proteins is defined as $\mu = \nu/E$, where ν is the protein terminal speed and E is the electric field strength. As there are no experimental values of μ for either MinD or MinE, we assume that they have the same type of free charges and define a new parameter J as

$$J_i = \mu_i E \equiv \frac{D_i J}{D_E} \ ,$$

where $i = \{D, d, E, e\}$. Initially, we assume that MinD and MinE are mainly at the opposite ends of the cell. The hard-wall boundary conditions are imposed at both ends of the bacterium.

V. RESULTS AND DISCUSSION

Exposure of biological cells to an electric field can lead to a variety of responses, both biophysical and biochemical. Here, we proposed a model of the response at the molecular level. Figure 3 shows space-time plots of the total MinD ($n_D^k + n_d^k$) concentration (above) and total MinE ($n_E^k + n_e^k$) (below) concentration for $J = 0.0$ μm/s to $J = 0.3$ μm/s and for (a) $N = 400$ and (b) $N = 1500$. Clearly, in the absence of the field ($J = 0.0$ μm/s), the MinD and the MinE oscillation patterns are in good agreement with the experimental results [9]; namely, MinE is more localized at midcell and then sweeps toward a cell pole, displacing MinD to localize at the poles. Once a MinE cluster reaches the cell pole, it disappears in the cytoplasm, only to reform at midcell where the process repeats, but at the other half of the cell. This process is repeated continuously, resulting in an oscillation of the Min protein.

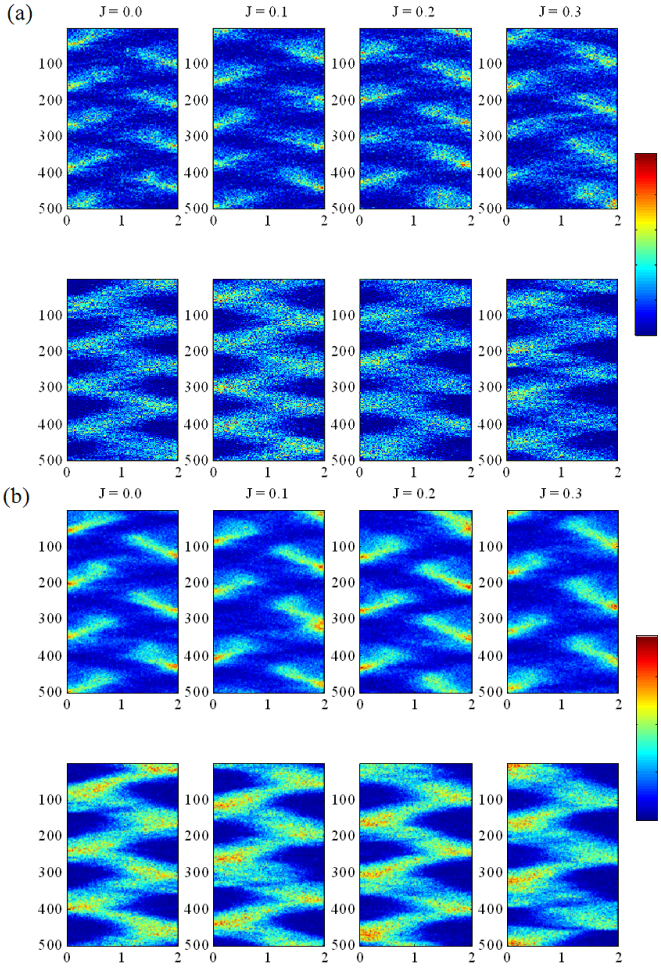

Fig. 3. Space-time plots of total ($n_D^k + n_d^k$) MinD (above) and total ($n_E^k + n_e^k$) MinE (below) concentrations for $J = 0.0$ μm/s to $J = 0.3$ μm/s where (a) $N = 400$ and (b) $N = 1500$. The color scale, running from blue to red, denotes an increase in the total numbers of Min proteins from lowest to highest. The vertical scale spans time for 500 s. Time increases from top to bottom. The horizontal scale spans a bacterial length of 2 μm. Note the increase in the MinD concentration at the right pole and that in the MinE concentration at the left pole.

When the external electric field is turned on ($J \neq 0$ μm/s), the oscillation patterns are no longer symmetric about the midcell. This is mainly because Min protein themselves are charged macromolecules (MinD, molecular weight = 29,936.61D and charge = 4.5e; MinE, molecular weight = 10,416.08 D and charge =

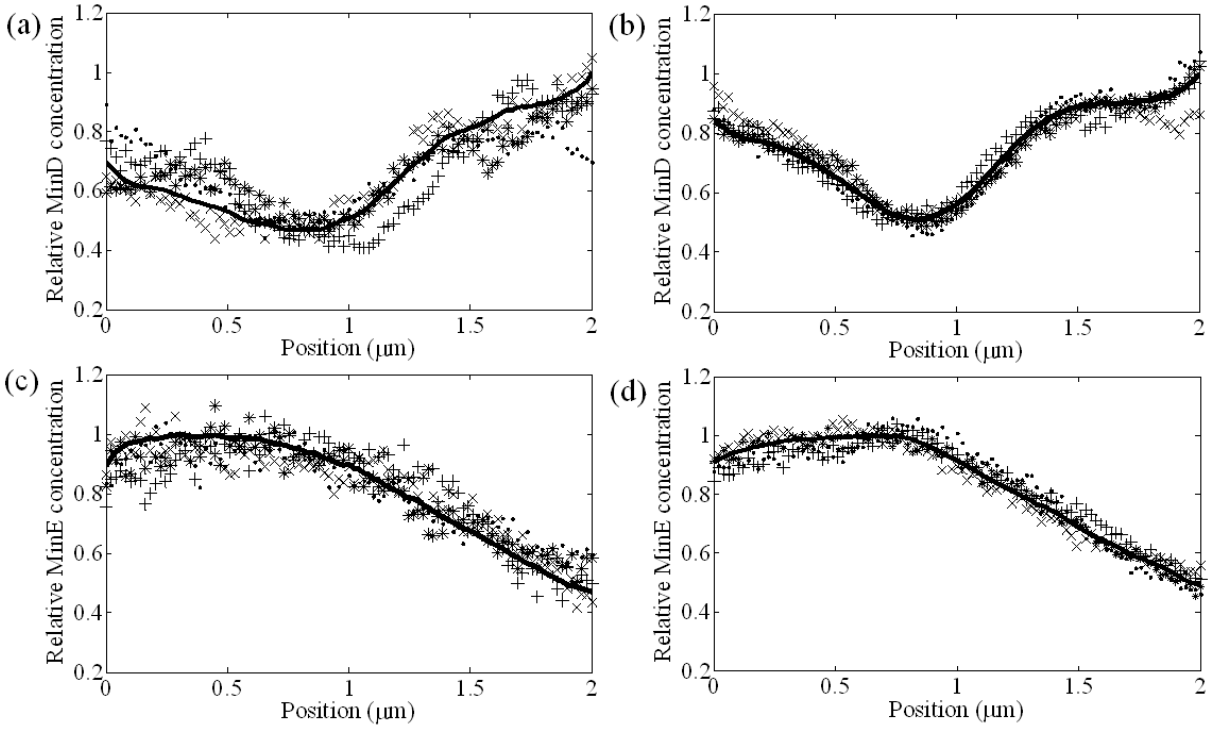

Fig. 4. Relative MinD concentrations (a) and (b) and relative MinE concentrations (c) and (d) as functions of x for $J = 0.3$ μm/s. In (a) and (c), $N = 400$ and in (b) and (d), $N = 1500$. Solid lines show averages over 15 successive cycles. The markers in the figures represent Min protein concentrations of four individual oscillation cycles.

0.5e; www.eolproject.org:8080/). Hence, when protein molecules are subject to the electric field, they will be pushed in a direction opposite to that of the field. In our simulation, we assume that MinD and MinE have the same types of charges and that the effect of the electric force on the Min proteins is modeled by a biased random walk (see Eq. (5)). Thus, it is quite obvious that the symmetry breaking of the oscillatory dynamics of Min protein may arise from an electric force that acts on the Min proteins or, equivalently, from the biased random walk that is used to model the diffusion process. Generally, membrane-bound proteins, like Min proteins, can have a variety of motions including Brownian motion, biased or directed motion, superdiffusion, and subdiffusion. These various motions influence greatly the kinetics of the reactions among these proteins. The mechanisms driving these motions may be, *e.g.*, obstruction by other proteins, transient binding, confinement by the membrane skeleton, and possible hydrodynamic interactions. Of course, an interaction like an external field could cause a more complicated and highly non-linear motion. Moreover, what could significantly happen as a result of this mentioned factor are transitions between transport modes *e.g.*, non-Gaussian diffusion. Whether the anomalous diffusion or other motion characteristics of proteins would show crossover with normal diffusion remains a key issue to be resolved. Better understanding of these mechanisms could improve our knowledge of protein mobility. Taking into account fluctuating forces that are colored rather than Gaussian-white forces allows more events like trapping or confined events to happen. These characteristics can equivalently be recast in the context of a distribution of the energy landscape. Knowing energy landscape, including the Hamiltonian and the symmetry, would certainly provide us more aspects to investigate Min protein dynamics. Experimentally, the energy landscape can be obtained by using a signal intensity analysis, *e.g.*, a tracking technique [67].

As the external field parameter J increases from 0.0 μm/s to 0.3 μm/s, the periods of the oscillations of both MinD and MinE increase approximately from 100 s to 150 s. The periods determined using our system are in good agreement with experiments, with periods of 30 – 120 s in the absence of the field [5]. In addition, we also calculate the period of the oscillation by using a linear stability analysis (see Appendix B); unfortunately, the result from the linear stability analysis shows a decrease in the period of the oscillation when J increases. The decease in the period of oscillation in the linear stability analysis may be caused by the linearization of the reaction terms in Eq. (1) - (4). Thus, the increase in the period of the oscillation in the Monte Carlo simulations must be caused by the nonlinearity of Eq. (1) - (4). With regards to fluctuation-driven instability, in the case of a low N, the stochastic fluctuated data have been found to be very far off from the average behavior or from those

results obtained from the deterministic model [9]. The noise involved has shifted the correct trend of the behavior of Min proteins. However, as a consequence of the robustness of the dynamics, the oscillatory pattern of the proteins still exists even though the number of Min proteins is relatively low.

In order to estimate the order of magnitude of the external field strength that can cause significant changes in the oscillatory behavior of Min proteins, we have used the value of ionic mobility (or electrophoretic mobility) μ from the gel-electrophoresis experiments of other proteins [68]. For proteins that have a diffusion coefficient with the same order of magnitude as that of the Min proteins, $D \approx 0.25 \times 10^{-12}$ m^2/s, $\mu \approx 2 \times 10^{-8}$ m^2/(V·s) [68]. From our simulation, the typical value of J that can significantly change the oscillatory behavior is $J = 0.3 \times 10^{-6}$ m/s, so the strength of electric field inside the *E. coli* cell is approximately $E = J/\mu = 15$ V/m or 0.15 V/cm. The next step is to convert the cytoplasmic field strength E to the external field strength E_0. From the detailed calculations shown in the Appendix A, we determined that the typical value of the external field strength to be $E_0 = E/1.078 = 0.14$ V/cm, which is very low when compared with the typical electroporetic field strength, which is on the order of 100 V/cm to 10 kV/cm [69]. Thus, an external field strength of $E \approx 0.14$ V/cm can cause abnormal division of *E. coli* cell and does not result in electroporation or membrane damage.

In Figure 4, the relative MinD and MinE concentrations as functions of x for $J = 0.3$ μm/s with $N = 400$ and $N = 1500$ are shown. The minima and the maxima of the MinD and the MinE concentrations, respectively, are significantly shifted from midcell ($x = 1$). Figure 1 also indicates that, although both MinD and MinE are pushed in the same direction by the electric field, they tend to be more concentrated at opposite ends when J is increased. A possible explanation is that MinD and MinE tend to repel each other, so in the absence of an electric field, the location of the minimum of the MinD concentration is at the location of the maximum MinE concentration. Moreover, although there is an electric force to push them in the same direction, this force cannot overcome the repulsion force between them. Fluctuations around the solid lines can be very large when N is small.

Figure 5 shows the relative concentration profiles of MinD (above) and MinE (below) as functions of position x along the bacterium length under the influence of an electric field with $J = 0.3$ μm/s at various total numbers of Min proteins. It shows that the position of the global minimum of MinD and the position of the global maximum of MinE concentrations do not change as the total number of Min proteins is changed. This implies that only J controls these global extremum positions. Moreover, the values of the relative global minimum concentrations of the MinD protein appear to be lowered as N increases while the relative global maximum of MinE protein concentration is higher. These demonstrate the

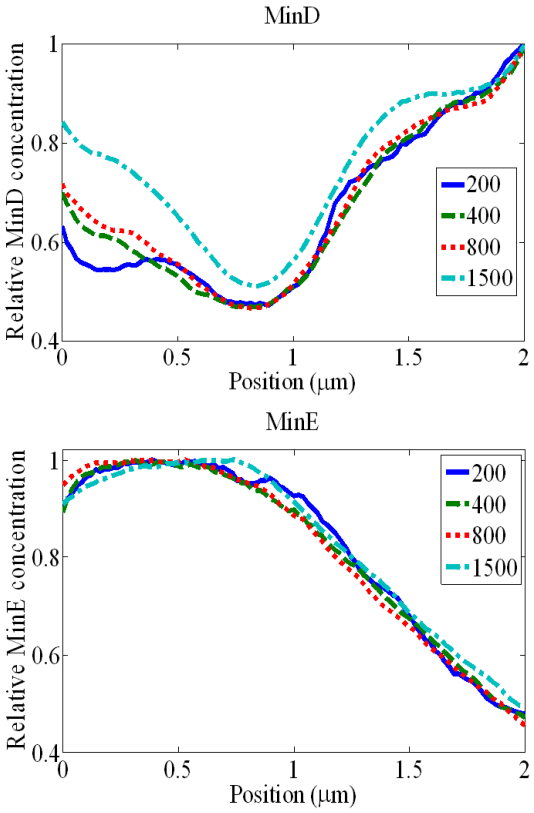

Fig. 5. Relative concentrations of MinD (above) and MinE (below) as functions of position x along the bacterium length under the influence of an electric field with $J = 0.3$ μm/s. The curves show that varying the total numbers of Min proteins does not change the MinD global minimum and the MinE global maximum concentration positions.

significance of using fewer protein copies that could result in the degradation of the accuracy not only of the extremum, but also of the central features. Of course, the correlation between the minimum and maximum is constrained by conservation of the total number of the both Min protein copies, but fluctuations set bounds on the concentration levels. These effects can also be discussed in the context of nucleoid occlusion [70]. In the absence of the field, the MinCDE system normally tends to prevent polar FtsZ rings because the nucleoids will inhibit FtsZ ring formation elsewhere except at midcell. The correlations between local and global minimum (maximum) of MinD (MinE) suggests that a high enough Min protein concentration will reduce the local minimum (maximum) effect, which is related to the probability of polar division in each single oscillator cycle. This leads us to believe that too low a concentration of Min proteins can result in an unacceptable probability of polar division. This may suggest that *E. coli* may be using the optimal number of Min proteins, trading off midpoint precision against the cost of protein synthesis [9]. This activity of *E. coli* is believed to be even more subtle when the situation is made more complicated by the presence

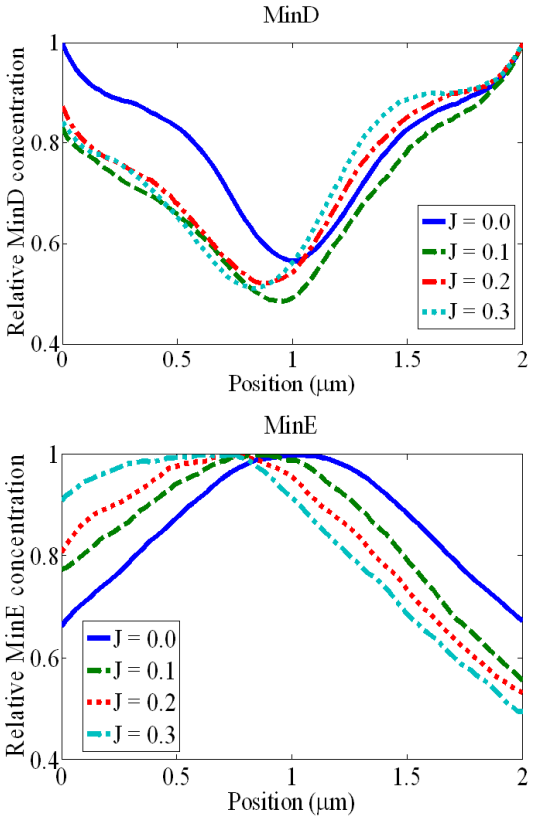

Fig. 6. Relative concentrations of MinD (above) and MinE (below) as functions of position x along the bacterium length under the influence of an electric field for $N = 1500$. The curve shows a shift, which depends on the strength of the field, in the local minima of MinD concentration and in the local maxima of MinE concentration from the midcell position.

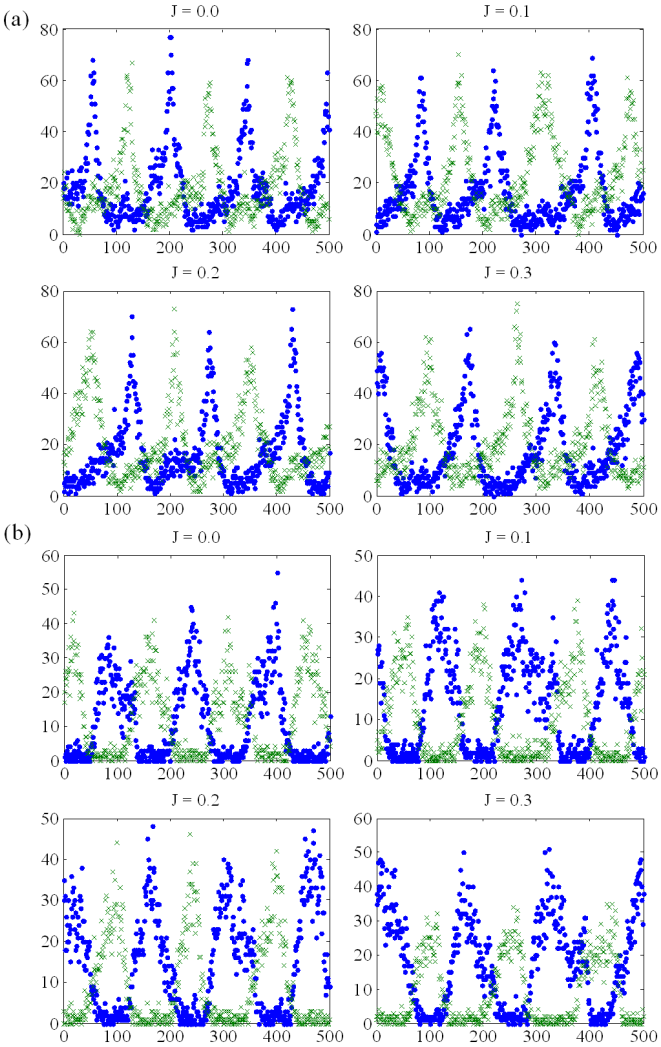

Fig. 7. Plots of concentrations of (a) MinD and (b) MinE protein. Plots are focused at the left end grid ($\cdot$) and the right end grid (x) as functions of time in seconds for $J = 0.0$ μm/s to $J = 0.3$ μm/s. The vertical scales denote numbers of protein copies in the system. The horizontal scale spans time for 500 s.

of an electric field.

Figure 6 shows relative concentrations of MinD (above) and MinE (below) as functions of position x along the bacterium length under the influence of an electric field for $N = 1500$. In the case of no external field ($J = 0.0$ μm/s), the relative concentrations of MinD and MinE are seen to be symmetric about the midcell. MinD has a minimum at midcell whereas MinE has a maximum, which is in good agreement with previous studies [9]. When the external electric field is turned on, a shift in the minimum and the maximum of the MinD and the MinE concentrations, respectively, is once again observed to be J dependent. Both the positions of the MinD concentration minimum and the MinE concentration maximum are more pronouncedly shifted towards the left pole as J increases. The minimum of MinD and the maximum of MinE concentrations are noted to be always shifted to the left pole. This difference arises because of the relative magnitudes of the forces acting on the two proteins. There is a repulsive force between the MinD and the MinE proteins, and in the absence of any other force, this explains why the location of the maximum of MinE concentration is at the location of the minimum of the MinD concentration. When an external field is applied (as expressed by a non-zero value of J), then one must take into account the relative magnitudes of the two forces. These results are consistent, at least qualitatively, with those obtained with a previously proposed deterministic partial differential model [16].

Figures 7(a) and (b) shows that the concentrations of MinD and MinE at the left end grid and the right end grid versus time, respectively. It is easy to see that when $J = 0.0$ μm/s, the concentrations of MinD (or MinE) at the left end and the right end grids have the same patterns of oscillations with the same frequencies and amplitudes, but with a phase difference of 180°. When an external field is applied, the amplitudes of the oscil-

lations at the two end grids are no longer equal. As J is increased, the amplitude of the oscillation of MinD at the left end grid decreases while that of MinE increases.

VI. CONCLUDING REMARKS

Proper divisions of bacteria require accurate definition of the division site. This accurate identification of the division site is determined by the rapid pole-to-pole oscillations of MinCDE. We have used a stochastic model to study the effects of an external electric field and noise on the *E. coli* MinCDE system. The stochastic approach is motivated by previous studies on how intrinsic chemical fluctuations in spatially extended systems can give rise to properties that are radically different from what would be described by using a mean-field model [16]. The model itself has been modified from that of Ref. 9.

We found that, if strong enough, an external electric field can shift the positions of the MinD concentration minimum and the MinE concentration maximum from midcell region. This shift appears to depend on the strength of the electric field. We also found that the effects of an electric field did not depend on the total number of Min proteins in *E. coli*. The results from the application of this stochastic model are, at least qualitatively, consistent with those obtained by using our deterministic model [16]. With regards to the fluctuation-driven instability, it was shown that, in the case of low N, the stochastically fluctuated data could be very far off from the average behavior or from the results obtained by using a deterministic model. The noise involved shifted the correct trend of Min protein behavior. However, as a consequence of the robustness of the dynamics, the oscillatory pattern of the proteins still existed even though the number of Min proteins was relatively low. When considering the correlations between local and global minimum (maximum) of MinD (MinE), our results suggests that using a high enough Min protein concentration will reduce the local minimum (maximum) effect, which is related to the probability of polar division in each single oscillator cycle. This leads us to believe that too low a concentration of Min proteins can result in an unacceptable probability of polar division.

APPENDIX A

In order to study the dielectric properties of *E. coli*, Holzel [61] proposed a three-shell spherical model in which the cell membrane is modeled as three dielectric spherical shells, equal inner and outer membranes with thicknesses of 11 nm and a periplasmic with a thickness of 50 nm. The relative permittivities of the cytoplasm, inner membrane, perils, outer membrane, and suspending medium were found to be 60, 3, 60, 3 and 78, respectively. In order to determine the relationship between

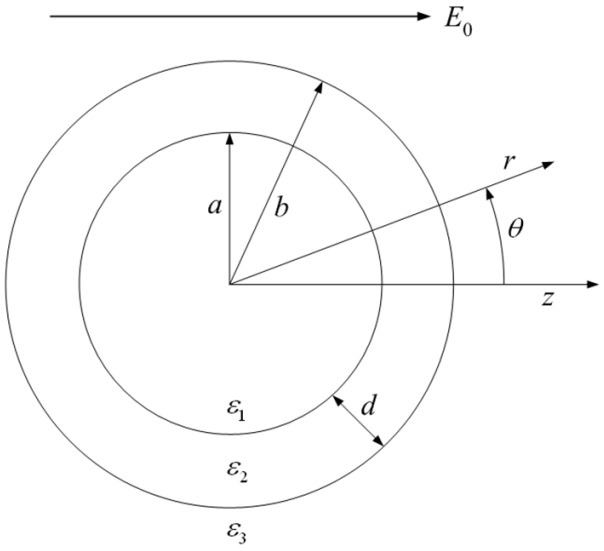

Fig. 8. Spherical shell model of *E. coli*.

the applied field E_0 and the field strength E inside the cytoplasm of *E. coli*, we also use the model proposed by Holzel [61] to represent *E. coli* cell. However, for the sake of simplicity, rather than considering the cell membrane as consisting of three spherical shells, we model it as a single spherical shell as shown in Figure 8. The spherical cell volume is considered to have inner and outer radii a and b, respectively, and a membrane thickness d. The relative permittivities of the cytoplasm, cell membrane and external medium are ε_1, ε_2 and ε_3, respectively. The relative permittivity of the cell membrane ε_2 is approximated to be the averaged value of relative permittivity of the three shells; namely, $\varepsilon_2 = (11 \cdot 3 + 50 \cdot 60 + 11 \cdot 3) / (11 + 50 + 11) = 42.58$. Φ_1, Φ_2 and Φ_3 denote the potentials in the three regions. The constant electric field E_0 is applied in the z-direction.

With the boundary condition that Φ must be finite at $r = 0$ and $\vec{E}$ is the uniform field at large distances, the potential at different regions must be of the form

$$\Phi_1(r,\theta) = \sum_{l=0}^{\infty} A_l r^l P_l(\cos\theta) \ ,$$

$$\Phi_2(r,\theta) = \sum_{l=0}^{\infty} \left[B_l r^l + \frac{C_l}{r^{l+1}} \right] P_l(\cos\theta) \ ,$$

$$\Phi_3(r,\theta) = -E_0 r + \sum_{l=0}^{\infty} \frac{D_l}{r^{l+1}} P_l(\cos\theta) \ , \qquad \text{(A1)}$$

and the boundary conditions at $r = a$ and $r = b$ yield

$$\Phi_1(a,\theta) = \Phi_2(a,\theta) \ ,$$
$$\Phi_2(b,\theta) = \Phi_3(b,\theta) \ ,$$
$$\varepsilon_1 \frac{\partial \Phi_1}{\partial r} \mid_{r=a} = \varepsilon_2 \frac{\partial \Phi_2}{\partial r} \mid_{r=a} \ ,$$
$$\varepsilon_2 \frac{\partial \Phi_2}{\partial r} \mid_{r=b} = \varepsilon_3 \frac{\partial \Phi_3}{\partial r} \mid_{r=b} \ .$$

These four conditions, which hold for all angles θ, are sufficient to determine the unknown constant in Eq. (A1). All coefficients with $l \neq 1$ vanish. The problem is now well defined and yields the following expression for the potential in the cytoplasm:

$$\Phi_1(r,\theta) = -\frac{9b^3 E_0 \varepsilon_2 \varepsilon_3}{\varepsilon((2a^3+b^3)\varepsilon_2 + 2(-a^3+b^3)\varepsilon_3) + 2\varepsilon_2((-a^3+b^3)\varepsilon_2 + (a^3+2b^3)\varepsilon_3)} r\cos\theta \ . \tag{A2}$$

With parameter values $\varepsilon_1 = 60$, $\varepsilon_2 = 42.58$, $\varepsilon_3 = 78$, $b = 2.0$ μm, $d = 72$ nm, Eq. (A2) becomes

$$\Phi_1 = -1.078 E_0 r\cos\theta = -1.078 E_0 z \ ,$$

and the corresponding electric field inside the cytoplasm is

$$E = E_{1z} = -\frac{\partial \Phi_1}{\partial z} = 1.078 E_0 \ . \tag{A3}$$

We also used other values of radius b in the range 1-3 μm, but the ratio E_{1z}/E_0 did not change significantly from the value of 1.078. It should be noted that in a more realistic model of *E. coli*, the cross section should be an ellipsoid instead of a sphere. However, using the ellipsoid model would make the estimation even more complicated.

APPENDIX B

If we want to determine weather the steady state is stable against small spatial perturbations, we can do this by using a linear stability analysis. First, we write our set of equations, Eqs. (1) - (4), in the form

$$\frac{\partial \vec{\rho}}{\partial t} = \mathbf{D}\frac{\partial^2 \vec{\rho}}{\partial x^2} + \mathbf{J_E}\frac{\partial \vec{\rho}}{\partial x} + \vec{f}(\vec{\rho}) \ , \tag{B1}$$

where $\vec{\rho}$ is the Min proteins density vector, $\mathbf{D}$ is a diffusion matrix, $\mathbf{J_E}$ is an external field matrix, and $\vec{f}(\vec{\rho})$ is a nonlinear function of $\vec{\rho}$. Suppose $\vec{\rho}^*$ is a homogeneous fixed point of Eq. (B1), then we define

$$\vec{\rho} \equiv \delta\vec{\rho} + \vec{\rho}^* \ , \tag{B2}$$

where $\delta\vec{\rho}$ is a small variation from the fixed point. Substituting Eq. (B2) in Eq. (B1), we get

$$\frac{\partial \delta\vec{\rho}}{\partial t} = \mathbf{D}\frac{\partial^2 \delta\vec{\rho}}{\partial x^2} + \mathbf{J_E}\frac{\partial \delta\vec{\rho}}{\partial x} + \vec{f}(\vec{\rho}^* + \delta\vec{\rho}) \tag{B3}$$

Then, we take a multivariate Taylor expansion of $\vec{f}(\vec{\rho}^* + \delta\vec{\rho})$ around a homogeneous fixed point $\vec{\rho}^*$:

$$\begin{aligned}\vec{f}(\vec{\rho}^* + \delta\vec{\rho}) &= \vec{f}(\vec{\rho}^*) + \frac{\partial \vec{f}}{\partial \vec{\rho}}|_{\vec{\rho}^*}\,\delta\vec{\rho} + \ldots \\ &= \frac{\partial \vec{f}}{\partial \vec{\rho}}|_{\vec{\rho}^*}\,\delta\vec{\rho} + \ldots \\ &= \mathbf{J}^*\delta\vec{\rho} + \ldots \ ,\end{aligned} \tag{B4}$$

where $\mathbf{J}^*$ is the Jacobian matrix evaluated at the fixed point $\vec{\rho}^*$ and the Jacobian matrix is defined as

$$\mathbf{J} = \begin{bmatrix} \frac{\partial f_1}{\partial \rho_1} & \frac{\partial f_1}{\partial \rho_2} & \cdots & \frac{\partial f_1}{\partial \rho_n} \\ \frac{\partial f_2}{\partial \rho_1} & \frac{\partial f_2}{\partial \rho_2} & \cdots & \frac{\partial f_2}{\partial \rho_n} \\ \vdots & \vdots & & \vdots \\ \frac{\partial f_n}{\partial \rho_1} & \frac{\partial f_n}{\partial \rho_2} & \cdots & \frac{\partial f_n}{\partial \rho_n} \end{bmatrix} \ .$$

For a small variation from the fix point, only the first term in Eq. (B4) is significant. If we want to know how trajectories behave near the equilibrium point, *e.g.*, whether they move toward or away from the equilibrium point, it should, therefore, be good enough to keep just this term. Then, we have

$$\vec{f}(\vec{\rho}^* + \delta\vec{\rho}) = \mathbf{J}^*\delta\vec{\rho} \ . \tag{B5}$$

Substituting Eq. (B5) in Eq. (B3), we obtain

$$\frac{\partial \delta\vec{\rho}}{\partial t} = \mathbf{D}\frac{\partial^2 \delta\vec{\rho}}{\partial x^2} + \mathbf{J_E}\frac{\partial \delta\vec{\rho}}{\partial x} + \mathbf{J}^*\delta\vec{\rho} \ . \tag{B6}$$

Since the matrix $\mathbf{J}^*$ is a constant matrix, this is just a set of linear differential equations. Now, suppose the solution is in the form

$$\delta\vec{\rho} = \delta\vec{\rho}_0 e^{\omega t} e^{iqx} \ . \tag{B7}$$

Substituting Eq. (B7) in Eq. (B6), we have

$$\omega\delta\vec{\rho} = -\mathbf{D}q^2\delta\vec{\rho} + iq\mathbf{J_E}\delta\vec{\rho} + \mathbf{J}^*\delta\vec{\rho}$$

Thus, ω is just an eigenvalue of the equation

$$(-\mathbf{D}q^2 + iq\mathbf{J_E} + \mathbf{J}^*)\delta\vec{\rho} = \omega\delta\vec{\rho} \ . \tag{B8}$$

The real part of ω will determine weather the equations is linearly stable under a small spatial perturbation whereas its imaginary part will determine the period of the oscillation,

$$T = \frac{2\pi}{\mathrm{Im}(\omega)} \ . \tag{B9}$$

If we know that there exists only one eigenvalue ω whose real part is positive, then we can conclude that this homogeneous fixed point is linearly unstable under a small spatial perturbation.

We use an iterative method to find the homogeneous fixed point of our set of equations, Eq. (1)-(4). We did the iterative method several times with different starting

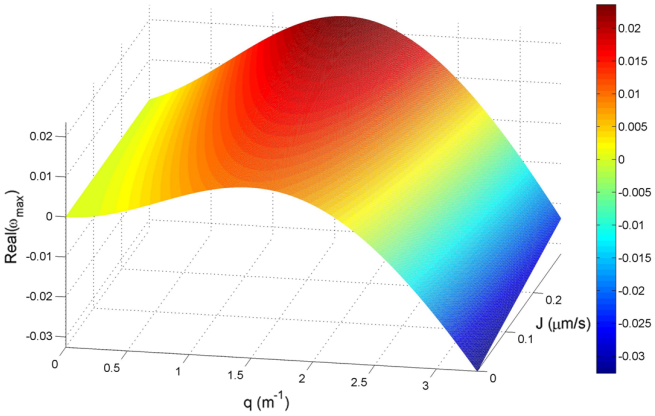

Fig. 9. Plot of the maximum real part of the eigenvalue ω as a function of wavenumber q and external electric field parameter J. The figure shows that the Min protein system is prefers the oscillatory dynamics more when the strength of the applied field is increased.

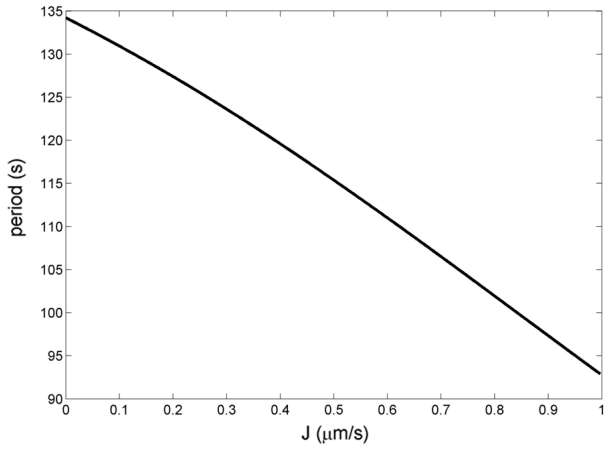

Fig. 10. Period of the oscillation obtained by using Eq. (B9).

points, but we only found one fixed point,namely, $\rho_D = 747.06$, $\rho_E = 0.00$, $\rho_d = 2.94$ and $\rho_e = 750.00$. With this fixed point, together with Eq. (B8), we are able to find the eigenvalues ω and determine if, for a certain parameter space, the fixed point is linearly stable.

Figure 9 show the maximum real part of ω as a function of wavenumber q and electric field parameter J. For $J = 0$ the positive real part of ω is maximized when $q \approx 1.5$ m^{-1}. This indicates the presence of a maximally linearly unstable oscillating mode with a wavelength of 4.2 mm [6]. When J increase, the maximum real part of ω is increase too, but the corresponding wavenumber is unchanged. This indicates that when the external electric field is applied, the linearly unstable oscillating dynamics is stronger. The existence of the linear instability in Eq. (1)-(4) is crucial, since it means that the oscillating pattern will spontaneously generate itself from a variety of initial conditions including nearly homogeneous ones.

The period of the oscillation was calculated by using Eq. (B9) where ω here is the eigenvalue which has the maximum real part. Figure 10 is a plot between the period of the oscillation and the external field parameter J by using a linear stability analysis. We can see that when J increase the period of the oscillation is decease which is contradict to the Monte Carlo simulation results. This contradiction may be caused by the nonlinearity of the reaction terms in our system of equations. When we do a linear stability analysis, these terms are linearized to only the first order but the increase of the period of the oscillation may largely depend on the nonlinearity, so the linearization of the equations may give an inaccurate results.

ACKNOWLEDGMENTS

This work was supported by the National Center for Genetic Engineering and Biotechnology (BIOTEC), The Thailand Research Fund (TRF), The Commission on Higher Education, Institut de Recherche Pour le Development (IRD), The Software Industry Promotion Agency (Public Organization), Strategic Scholarships for Frontier Research Network, Postgraduate Education and Research Program in Chemistry (PERCH-CIC) and The Thai Center of Excellence for Physics (Integrated Physics Cluster).

REFERENCES

[1] P. A. de Boer, R. E. Crossley and L. I. Rothfield, Cell **56**, 641 (1989).
[2] Z. Hu and J. Lutkenhaus, Mol. Microbiol. **34**, 82 (1999).
[3] Z. Hu and J. Lutkenhaus, J. Bacteriol. **182**, 3965 (2000).
[4] P. A. de Boer, R. E. Crossley and L. I. Rothfield, J. Bacteriol. **174**, 63 (1992).
[5] D. M. Raskin and P. A. de Boer, Proc. Natl. Acad. Sci. U.S.A. **96**, 4971 (1999).
[6] M. Howard, A. D. Rutenberg and S. de Vet, Phys. Rev. Lett. **87**, 278102 (2001).
[7] H. Meinhardt and P. A. de Boer, Proc. Natl. Acad. Sci. U.S.A. **98**, 14202 (2001).
[8] K. Kruse, Biophys. J. **82**, 618 (2002).
[9] M. Howard and A. D. Rutenberg, Phys. Rev. Lett. **90**, 128102 (2003).
[10] K. C. Huang, Y. Meir and N. S. Wingreen, Proc. Natl. Acad. Sci. U.S.A. **100**, 12724 (2003).
[11] D. Fange and J. Elf, PLoS. Comput. Biol. **2**, e80 (2006).
[12] R. A. Kerr, H. Levine, T. J. Sejnowski and W. J. Rappel, Proc. Natl. Acad. Sci. U.S.A. **103**, 347 (2006).
[13] N. Pavin, H. C. Paljetak and V. Krstic, Phys. Rev. E **73**, 21904 (2006).
[14] F. Tostevin and M. Howard, Phys. Biol. **3**, (2006).
[15] W. Ngamsaad, W. Triampo, P. Kanthang, I. M. Tang, N. Nuttawut, C. Modchang and Y. Lenbury, J. Korean Phys. Soc. **46**, 1025 (2005).

[16] C. Modchang, P. Kanthang, W. Triampo, W. Ngamsaad, N. Nuttawut, I. M. Tang, S. Sanguansin, A. Boondirek and Y. Lenbury, J. Korean Phys. Soc. **46**, 1031 (2005).
[17] T. Simonson, Rep. Prog. Phys. **66**, 737 (2003).
[18] M. Zhao, J. V. Forrester and C. D. McCaig, Proc. Natl. Acad. Sci. U.S.A. **96**, 4942 (1999).
[19] J. Gerhart, M. Danilchik, T. Doniach, S. Roberts, B. Rowning and R. Stewart, Development **107**, 37 (1989).
[20] C. E. Helmstetter, Proc. Natl. Acad. Sci. U.S.A. **94**, 10195 (1997).
[21] J. M. Denegre, J. M. Valles, K. Lin, W. B. Jordan and K. L. Mowry, Proc. Natl. Acad. Sci. U.S.A. **95**, 14729 (1998).
[22] D. C. Henderson, S. R. Bisgrove, W. E. Hable, L. Alessa and D. L. Kropf, Protoplasma **203**, 112 (1998).
[23] K. R. Robinson, J. Cell Biol. **101**, 2023 (1985).
[24] B. Song, M. Zhao, J. V. Forrester and C. D. McCaig, Proc. Natl. Acad. Sci. U.S.A. **99**, 13577 (2002).
[25] E. D. Kirson, Z. Gurvich, R. Schneiderman, E. Dekel, A. Itzhaki, Y. Wasserman, R. Schatzberger and Y. Palti, Cancer Res **64**, 3288 (2004).
[26] J. C. Weaver and R. D. Astumian, Science **247**, 459 (1990).
[27] L. F. Jaffe, Soc. Gen. Physiol. Ser. **33**, 199 (1979).
[28] R. B. Borgens, J. W. Vanable Jr and L. F. Jaffe, J. Exp. Zool. **200**, 403 (1977).
[29] L. F. Jaffe and M. M. Poo, J. Exp. Zool. **209**, 115 (1979).
[30] R. B. Borgens, E. Roederer and M. J. Cohen, Science **213**, 611 (1981).
[31] G. H. Kenner, E. W. Gabrielson, J. E. Lovell, A. E. Marshall and W. S. Williams, Calcified. Tissue Int. **18**, 111 (1975).
[32] M. S. Cooper and R. E. Keller, Proc. Natl. Acad. Sci. U.S.A. **81**, 160 (1984).
[33] M. S. Cooper and M. Schliwa, J. Neurosci. Res. **13**, 223 (1985).
[34] P. W. Luther, H. B. Peng and J. J. C. Lin, Nature **303**, 61 (1983).
[35] S. H. Young and M. Poo, Nature **304**, 161 (1983).
[36] J. Teissie, V. P. Knutson, T. Y. Tsong and M. D. Lane, Science **216**, 537 (1982).
[37] U. Zimmermann and J. Vienken, J. Membrane Biol. **67**, 165 (1982).
[38] D. E. Knight and P. F. Baker, J. Membrane Biol. **83**, 147 (1985).
[39] W. A. Hamilton and A. J. H. Sale, Biochim. Biophys. Acta. **148**, 789 (1967).
[40] H. Hulsheger and E. G. Niemann, Radiat. Environ. Bioph. **18**, 281 (1980).
[41] R. Goodman, C. A. Bassett and A. S. Henderson, Science **220**, 1283 (1983).
[42] D. W. Bawcom, L. D. Thompson, M. F. Miller and C. B. Ramsey, J. Food Protect. **58**, 35 (1995).
[43] A. M. Rajnicek, C. D. McCaig and N. A. R. Gow, J. Bacteriol. **176**, 702 (1994).
[44] S. Palaniappan, S. K. Sastry and E. R. Richter, J. Food Process. Pres. **14**, 383 (1990).
[45] U. Zimmermann, G. Pilwat, F. Beckers and F. Riemann, Bioelectrochem. Bioenerg. **3**, 58 (1976).
[46] U. Zimmermann, G. Pilwat and F. Riemann, Biophys. J. **14**, 881 (1974).
[47] P. R. Gascoyne, R. Pethig, J. P. Burt and F. F. Becker, Biochim. Biophys. Acta. **1149**, 119 (1993).
[48] P. R. C. Gascoyne, J. Noshari, F. F. Becker and R. Pethig, IEEE. T. Ind. Appl. **30**, 829 (1994).
[49] J. Gimsa, P. Marszalek, U. Loewe and T. Y. Tsong, Biophys. J. **60**, 749 (1991).
[50] Y. Huang and R. P. Holzel, Phys. Med. **37**, 1499 (1992).
[51] Y. Huang, X. B. Wang, F. F. Becker and P. R. Gascoyne, Biochim. Biophys. Acta. **1282**, 76 (1996).
[52] Y. Huang, X. B. Wang, P. R. C. Gascoyne and F. F. Becker, Biochim. Biophys. Acta. **1417**, 51 (1999).
[53] J. Yang, Y. Huang, X. Wang, X. B. Wang, F. F. Becker and P. R. C. Gascoyne, Biophys. J. **76**, 3307 (1999).
[54] P. R. C. Gascoyne, X. B. Wang, Y. Huang and F. F. Becker, IEEE. T. Ind. Appl. **33**, 670 (1997).
[55] R. Pethig and G. H. Markx, Trends Biotechnol. **15**, 426 (1997).
[56] J. Yang, Y. Huang, X. B. Wang, F. F. Becker and P. R. C. Gascoyne, Biophys. J. **78**, 2680 (2000).
[57] K. Asami, Prog. Polym. Sci. **27**, 1617 (2002).
[58] A. Bonincontro and G. Onori, Chem. Phys. Lett. **398**, 260 (2004).
[59] F. Bordi, C. Cametti and T. Gili, J. Non-Cryst. Solids **305**, 278 (2002).
[60] K. Asami, T. Hanai and N. Koizumi, Biophys. J. **31**, 215 (1980).
[61] R. Holzel, Biochim. Biophys. Acta. **1450**, 53 (1999).
[62] S. L. Rowland, X. Fu, M. A. Sayed, Y. Zhang, W. R. Cook and L. I. Rothfield, J. Bacteriol. **182**, 613 (2000).
[63] J. Huang, C. Cao and J. Lutkenhaus, J. Bacteriol. **178**, 5080 (1996).
[64] D. M. Raskin and P. A. de Boer, J. Bacteriol. **181**, 6419 (1999).
[65] M. B. Elowitz, M. G. Surette, P. E. Wolf, J. B. Stock and S. Leibler, J. Bacteriol. **181**, 197 (1999).
[66] Y. L. Shih, X. Fu, G. F. King, T. Le and L. Rothfield, Embo J. **21**, 3347 (2002).
[67] U. Junthorn, S. Unai, P. Kanthang, W. Ngamsaad, C. Modchang, W. Triampo, C. Krittanai, D. Triampo and Y. Lenbury, J. Korean Phys. Soc. **52**, 639 (2008).
[68] U. Bohme and U. Scheler, Chem. Phys. Lett. **435**, 342 (2007).
[69] K. H. Schoenbach, F. E. Peterkin, R. W. Alden Iii and S. J. Beebe, IEEE. T. Plasma Sci. **25**, 284 (1997).
[70] X. C. Yu and W. Margolin, Mol. Microbiol. **32**, 315 (1999).